Cell Death and Differentiation (2012) 19, 1080–1089

www.nature.com/cdd

Somatic gonad sheath cells and Eph receptor signaling promote germ-cell death in *C. elegans*

X Li[1,3,5], RW Johnson[1,5], D Park[1,4], I Chin-Sang[2] and HM Chamberlin*[,1]

Programmed cell death eliminates unwanted cells during normal development and physiological homeostasis. While cell interactions can influence apoptosis as they do other types of cell fate, outside of the adaptive immune system little is known about the intercellular cues that actively promote cell death in healthy cells. We used the *Caenorhabditis elegans* germline as a model to investigate the extrinsic regulators of physiological apoptosis. Using genetic and cell biological methods, we show that somatic gonad sheath cells, which also act as phagocytes of dying germ cells, promote death in the *C. elegans* germline through VAB-1/Eph receptor signaling. We report that the germline apoptosis function of VAB-1 impacts specific cell death pathways, and may act in parallel to extracellular signal-regulated kinase MAPK signaling. This work defines a non-autonomous, pro-apoptotic signaling for efficient physiological cell death, and highlights the dynamic nature of intercellular communication between dying cells and the phagocytes that remove them.
Cell Death and Differentiation (2012) **19,** 1080–1089; doi:10.1038/cdd.2011.192; published online 13 January 2012

Physiological apoptosis, or apoptosis of apparently healthy cells, is a process important for tissue development and homeostasis.[1] Dysregulation of physiological apoptosis has a role in the etiology of many diseases, including autoimmune disorders and cancer.[2] This dysregulation can occur within the core cell death pathway, but also in the signals that control the decision to die (for examples, see Gurzov and Eizirik[3] and Ruffin *et al.*[4]). Therefore, it is critical to understand the various ways in which healthy cells adopt an apoptotic cell fate.

Like many cell fate decisions, physiological apoptosis can be initiated in response to cell-extrinsic signals. Some of these signals maintain survival circuits within the cell. For example, removal of growth factors such as granulocyte–macrophage colony-stimulating factor[5] or disruption of integrin-mediated cell adhesion[6] can act as microenvironmental triggers of apoptosis. Other extrinsic cues actively promote cell death through the so-called murder pathways. A well-studied example involves Fas ligand activation of intracellular signaling cascades through death receptors of the tumor necrosis factor-α superfamily.[7] Thus, animals have evolved multiple regulatory mechanisms to allow precise physiological control over programmed cell death.

One mechanism by which extrinsic cues can mediate physiological apoptosis is through direct cell–cell interactions. A recent study found that the membrane-bound isoform of Fas ligand was able to induce apoptosis in a mouse model.[8] Additionally, natural killer T-lymphocytes were shown to induce caspase-dependent cell death in target cells by direct delivery of perforin and granzyme-A.[9] However, whereas we have a good understanding of some key pro-apoptotic pathways used by the mammalian immune system, less is known about the signals that promote apoptosis in other physiological contexts.

The nematode *Caenorhabditis elegans* is a powerful model system in which to study apoptosis. In particular, examination of cell death in the *C. elegans* germline has shed light on important facets of apoptosis, and its relationship to complex processes such as aging and the DNA-damage response.[10] In *C. elegans*, as germ cells progress through meiosis, approximately half undergo cell death, where it is hypothesized that their cytosolic components are reallocated to 'nurse' remaining oocytes.[11,12] This caspase-dependent cell death occurs in apparently healthy germ cells, and has been termed physiological apoptosis to distinguish it from other types of germ-cell deaths.[13] Although many genes required for germ-cell apoptosis are known, we have taken the approach to use the *C. elegans* germline as a model to study cell interactions important for physiological cell death, which are not well understood.

[1]Department of Molecular Genetics, The Ohio State University, Columbus, OH 43210, USA and [2]Department of Biology, Queen's University, Kingston, ON K7L 3N6, Canada
*Corresponding author: HM Chamberlin, Department of Molecular Genetics, Ohio State University, 629 Biological Sciences Building, 484 W 12th Avenue, Columbus, OH 43210, USA. Tel: +614 688 0043; Fax: +614 292 4466; E-mail: chamberlin.27@osu.edu
[3]Current address: Department of Orthopedic Surgery, University of California, San Francisco, CA 94110, USA.
[4]Current address: Centre for Molecular Medicine and Therapeutics, Vancouver, BC, V5Z 4H4, Canada.
[5]These authors contributed equally to this work.
Keywords: cell murder; assisted cell suicide; ephrin; oocyte; engulfment
Abbreviations: ERK, extracellular signal-regulated kinase; EphR, Eph receptor
Received 17.5.11; revised 07.11.11; accepted 07.11.11; Edited by E Baehrecke; published online 13.1.12

In this work, we report the discovery of a novel regulator of physiological apoptosis in the *C. elegans* germline. We describe a role for VAB-1/Eph receptor (EphR) signaling in the promotion of cell death, and present data exploring the link between VAB-1 and other genes and pathways that influence germline apoptosis. Further, we demonstrate that somatic sheath cells contacting the apoptotic region of the germline function to promote apoptosis, and find that VAB-1 and the sheath cells impact the same apoptotic decision. This work provides a previously unknown example of apoptosis regulation by Eph signaling, and highlights the importance of communication between dying cells and their surviving neighbors during a physiological apoptosis decision.

Results

VAB-1/Eph signaling promotes physiological germ-cell apoptosis. The bi-lobed *C. elegans* gonad is composed of a germline that is largely separated from other tissues by a single-cell layer of somatic gonad sheath cells. Each gonad arm is a U-shaped structure where mitotically dividing germ nuclei at the distal end migrate proximally toward the uterus as they progress into and through meiosis (Figure 1a). These nuclei exist within a syncytium and only fully cellularize during the last portion of meiosis and oocyte maturation, but are hereafter termed 'cells' for simplicity.[14]

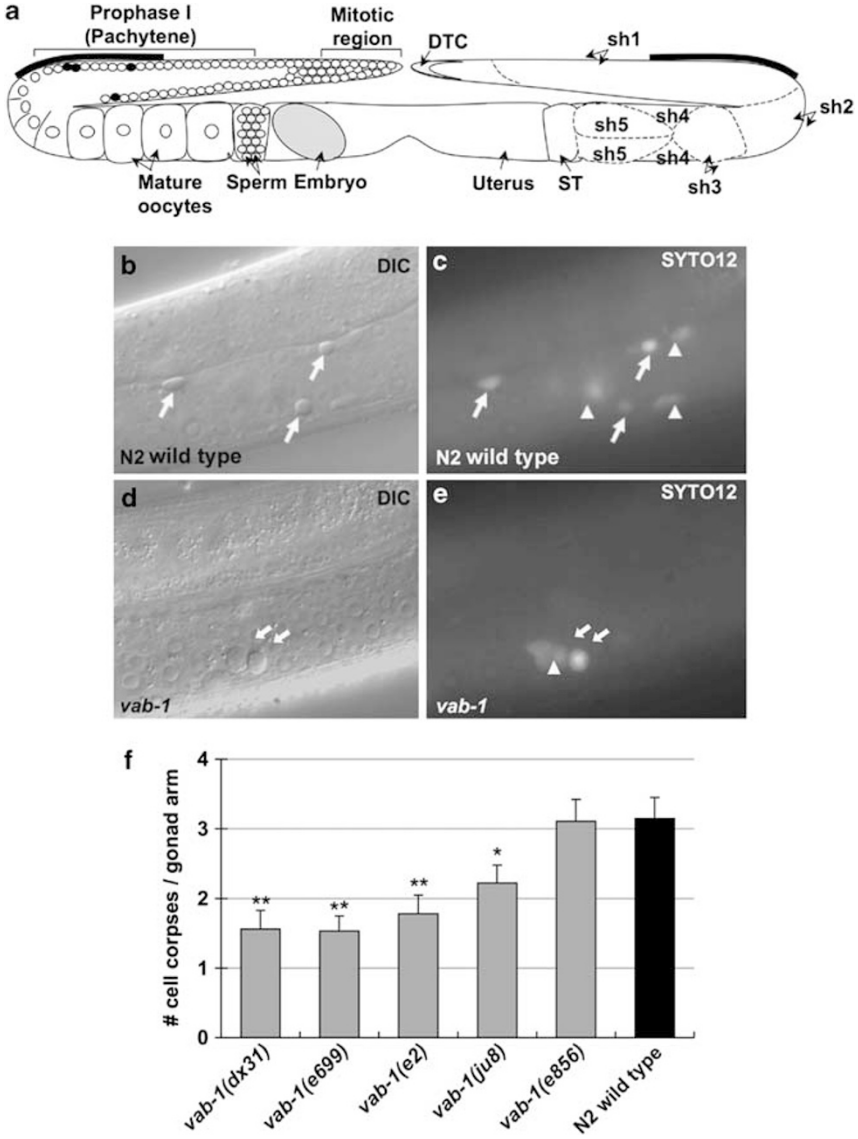

Figure 1 VAB-1/EphR signaling positively regulates physiological germline apoptosis. (**a**) Schematic of the *C. elegans* hermaphrodite gonad, highlighting germ-cell organization (left) and the somatic gonad, including the five sheath cell pairs (right). The primary region of germ-cell death is immediately distal to the loop (bars; ST, spermatheca; DTC, distal tip cell). (**b**–**e**) Nomarski differential interference contrast (DIC) and epifluorescence images of germlines from a wild-type strain N2 (**b**–**c**) and *vab-1(dx31)* mutants (**d** and **e**). Apoptotic germ-cell corpses (arrows) are observed as refractile, button-like discs under light microscopy, and/or preferentially stain with the fluorescent nucleic acid dye SYTO12 (arrows and arrowheads). (**f**) Germ-cell corpse counts among *vab-1* mutant strains (gray), as compared with the N2 wild type (black). Four of five mutant strains showed decreased germ-cell corpse numbers (49–71% of wild type; *n*: *dx31*, 40; *e699*, 32; *e2*, 37; *ju8*, 32; *e856*, 28; N2, 39; Mann–Whitney test with ties adjustment, $^{**}P<0.005$; $^{*}P=0.039$). Corpse count data are shown as mean ± S.E.M. from at least three independent experiments

Although physiological apoptosis in the *C. elegans* germline occurs in the absence of any cell-damaging stimuli, the frequency of germ-cell deaths can vary. The number of germ-cell corpses visible in a gonad arm at any given time is dependent upon factors that include animal age, oocyte quality regulators, and environmental stressors.[15,16] The discovery of molecular pathways responsive to some of these inputs reveals that regulation of germ-cell death is not strictly an autonomous process within the germline.[17–19] Concordantly, intercellular interactions are likely to exert some control over the rate of germ-cell death. However, we do not currently understand what molecules might mediate these physiological murder signals.

Extracellular signal-regulated kinase (ERK) signaling is required for many processes in the germline, including physiological apoptosis.[13] One can imagine a simple germ-cell murder signal to be a ligand–receptor interaction that impinges upon this pathway. We used a candidate approach to ask what intercellular signaling molecules might transduce such a signal; specifically, we asked whether any receptor tyrosine kinases (RTKs) might positively regulate physiological apoptosis. Expression of five RTKs is enriched in the *C. elegans* germline,[20] but only loss of VAB-1 EphR function was associated with a defect in germline apoptosis (Figures 1b–e). Four of five *vab-1* mutants tested showed 49–71% of the germ-cell corpse numbers observed in the wild-type strain N2 (Figure 1f). Notably, *vab-1(e2)* mutants, which carry a point mutation in the tyrosine kinase domain, and have the least amount of VAB-1 tyrosine phosphorylation in whole-worm lysates, showed a strong reduction in cell death.[21] These results indicate that forward signaling through VAB-1/EphR contributes to the frequency of physiological apoptosis.

The number of germ-cell corpses at any given time reflects multiple variables, including the total number of germ cells, the rate of cell death, and the rate of cell removal by engulfment. To ensure that the reduction in cell deaths observed under *vab-1(lf)* conditions was not a secondary consequence of a smaller germline, we quantified germ-cell numbers in *vab-1 (dx31)* mutants and N2 wild types. At 24 h after the mid-L4 larval stage, *vab-1* mutants had on average 448 germ cells as compared with 495 in N2 wild type (Figure 2a). In contrast to a typical *vab-1(dx31)* apoptosis frequency of 50–60%, the decrease in total cell number was only 9%, and was not statistically significant. We next analyzed *vab-1(dx31)*-null mutants in two engulfment-defective conditions. Both *vab-1 (dx31); ced-6(n1813)* double mutants and *vab-1(dx31); ced-10(RNAi)* animals showed decreases in germ-cell corpse numbers relative to wild-type controls. Together, these results verified the *vab-1* mutant phenotype as a germ-cell death, rather than a proliferation or engulfment, defect (Figure 2b). These engulfment defective conditions were used for select apoptosis experiments presented below.

To complement the quantification of cell death through corpse number counts, we used two additional means to identify dying cells: uptake of the vital dye SYTO12

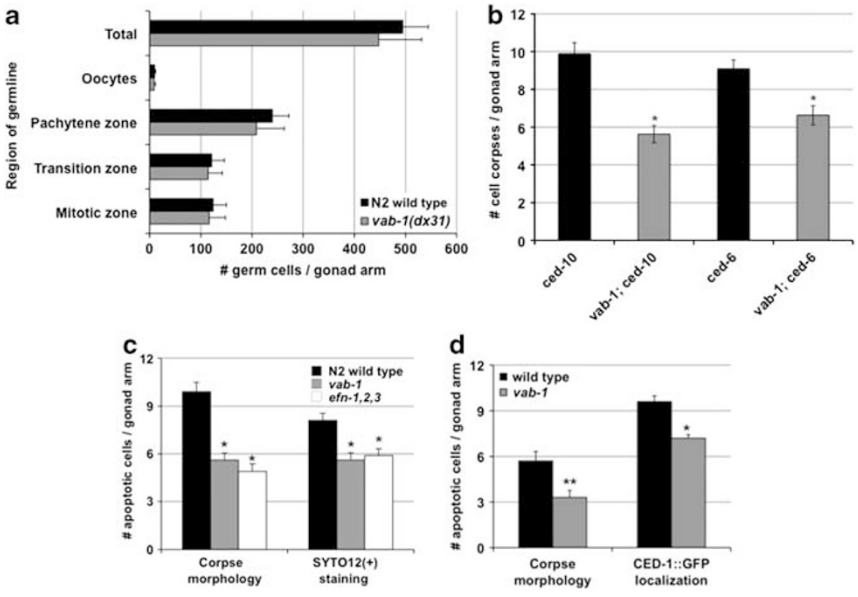

Figure 2 *vab-1* impacts germ-cell death by apoptosis promotion rather than suppression of proliferation or corpse engulfment. (**a**) Germ-cell quantification in N2 wild type and *vab-1(dx31)*-null mutants 24 h after mid-L4 larval stage. Loss of *vab-1* activity had no statistically significant impact on germ-cell numbers at any stage of development ($n = 10$). (**b**) Reduced germ-cell corpse counts in *vab-1(dx31)*-null strains under two cell engulfment-defective conditions, as compared with the wild type. (*n*: *ced-10(RNAi)*, 51; *vab-1;ced-10(RNAi)*, 52; *ced-6(n1813)*, 82; *vab-1;ced-6(n1813)*, 81; Student's *t*-test, $^*P < 0.001$). (**c**) Comparative quantification of apoptotic cells by means of corpse morphology under Nomarski DIC optics and preferential incorporation of the apoptotic body-specific fluorescent dye SYTO12. The numbers of SYTO12(+) cells were reduced in both *vab-1* ($n = 48$) and *efn* triple mutants (*efn-1,2,3*; $n = 45$) relative to the N2 wild type ($n = 52$; Student's *t*-test, $^*P < 0.001$). Experiments were performed under *ced-10(RNAi)* conditions. Mutations used: *efn-1(e96)*, *efn-2(ev658)*, *efn-3(ev696)*, and *vab-1(dx31).* (**d**) Comparative quantification of apoptotic cells by means of corpse morphology and epifluorescence of cells surrounded by the sheath cell-expressing phagocyte receptor reporter CED-1::GFP (*bcIs39*). *vab-1(dx31)*-null mutants showed a significant reduction in the number of germ cells encircled by the phagocyte receptor (*n*: wild type, 55; *vab-1*, 56; Student's *t*-test, $^*P < 0.01$; $^{**}P < 0.001$). CED-1::GFP cells were only scored positive when GFP localized around at least 75% of the germ-cell periphery. Data were collected from at least three independent experiments and represent the mean ± S.E.M.

and localization of the phagocyte receptor reporter CED-1::GFP.[13,22] Relative to wild type, *vab-1(dx31)* mutants showed a reduction in cell deaths according to both methods (Figures 2c and d). These results further confirmed that VAB-1/EphR stimulates physiological apoptosis in the *C. elegans* hermaphrodite germline.

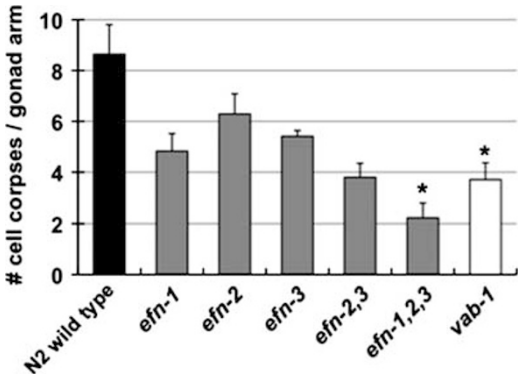

Figure 3 Three ephrin ligands have partially redundant pro-apoptotic functions. Germ-cell corpse quantification in strains carrying mutations in the genes for canonical ephrins, *efn-1*, *efn-2*, and *efn-3*. *efn-1,2,3* triple mutants show a strong germ-cell death defect, similar to *vab-1/EphR*-null mutants (*n*: N2 wild type, 35; *efn-1*, 41; *efn-2*, 22, *efn-3*, 25; *efn-2,3*, 25; *efn-1,2,3*, 35, *vab-1*, 40; Mann–Whitney test with ties adjustment, $*P<0.005$). Experiments were performed under *ced-10(RNAi)* conditions. Mutations used: *efn-1(e96)*, *efn-2(ev658)*, *efn-3(ev696)*, and *vab-1(dx31)*. Data are from at least three independent experiments and represent the mean ± S.E.M.

Sheath cell ephrins can signal to germline VAB-1 to promote apoptosis. EphR signaling is activated by a family of cell-surface ligands called ephrins. There are four named ephrins (EFNs) in *C. elegans*, and three of these (EFN-1,2,3) signal through VAB-1, whereas the divergent member of family, EFN-4, acts independent of VAB-1 during development, and is instead believed to signal through Semaphorin-signaling pathways.[21,23,24] Analysis of germ-cell death (under *ced-10(RNAi)* engulfment-defective conditions) in strains carrying mutations in the three canonical *efn* genes revealed variable pro-apoptotic activities, with the greatest degree of apoptosis reduction observed in *efn-1(e96) efn-2(ev658); efn-3(ev696)* triple mutants (Figures 2c and 3). As expected, germ-cell death was unaffected in *efn-4* mutant animals (data not shown). These data lend further evidence for an EphR signaling role in physiological germ-cell death, and implicate multiple EFN ligands in the partially redundant activation of VAB-1.

VAB-1 is expressed throughout the *C. elegans* germline, and localizes to germ-cell plasma membranes in the region of physiological apoptosis.[25] To confirm the pro-apoptotic function of *vab-1* in this tissue, we performed site-of-action experiments. Heterologous expression of VAB-1 in germ cells was able to rescue apoptosis in *vab-1(dx31)*; *ced-10(RNAi)* mutants (Figure 4a). Using *ced-6(n1813)* engulfment mutants, we also found that tissue-specific RNAi knockdown of *vab-1* in the germline, but not in the soma, recapitulated the apoptosis phenotype of *vab-1* genetic mutants (Figure 4b).

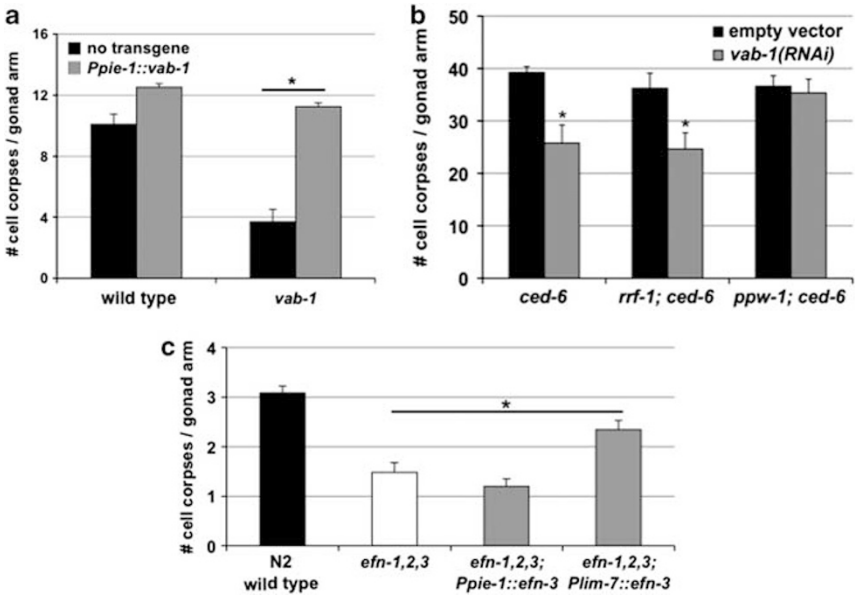

Figure 4 Germline VAB-1 function is necessary and sufficient to support normal levels of germ-cell death. (**a**) Germ-cell corpse counts in *ced-10(RNAi)* engulfment-defective animals carrying a transgene that directs the expression of VAB-1 under the control of the germline-specific promoter *pie-1* (P_{pie-1}::*vab-1*). Germline expression of P_{pie-1}::*vab-1* rescues the apoptosis deficit in *vab-1(dx31)* mutants (*n*: wild type, 21; *tnIs13*, 19; *vab-1*, 29; *vab-1; tnIs13*, 12; Student's *t*-test, $*P<0.001$). (**b**) Cell corpse counts in the germline of *ced-6(n1823)* engulfment-defective animals subjected to RNAi knockdown of endogenous *vab-1*. Attenuated *vab-1* activity by RNAi recapitulates the cell death phenotype of genetic *vab-1* mutants in wild-type animals (*n*: empty vector, 39; *vab-1(RNAi)*, 44) as well as in *rrf-1(pk1417)* mutant animals that retain RNAi activity in the germline, but lack it in the soma (*n*: empty vector, 24; *vab-1(RNAi)*, 31; Student's *t*-test, $*P<0.001$). Cell death is unaffected in *ppw-1* mutant animals in which RNAi knockdown functions only in the soma (*vab-1* expression is retained in the germline; *n*: empty vector, 31; *vab-1(RNAi)*, 31). (**c**) Cell corpse counts in *efn-1,2,3* triple mutants (normal engulfment) carrying transgenes that direct heterologous expression of *efn-3* cDNA. Expression of *efn-3* in the gonad sheath cells (P_{lim-7}::*efn-3*), but not the germline (P_{pie-1}::*efn-3*), partially rescued the germ-cell death defect in the *efn* triple mutant animals ($n=35$; Mann–Whitney test with ties adjustment, $*P=0.001$). All graphs summarize data from at least three independent experiments and represent the mean ± S.E.M.

Thus, *vab-1* activity in the germline was necessary and sufficient to promote germ-cell death. In addition, expression of EFN-3 in the gonad sheath cells partially rescued the apoptosis defect in *efn-1 efn-2; efn-3* triple mutants, but did not rescue when expressed in the germline (wild-type background; Figure 4c). Altogether, our data suggest a model where VAB-1 in the germline syncytium is signaled to by EFN ligands anchored within the sheath cell membrane.

VAB-1 does not mediate all intercellular pathways of germline apoptosis. The frequency of physiological germ-cell deaths is subject to many biological and environmental conditions. An example of such regulatory control is the increase in apoptosis that is observed as adult germlines begin to age.[13] One can observe the biological importance of such control, as physiological apoptosis has been shown to maintain oocyte quality in aging hermaphrodites.[26] Somatic signaling pathways that control aging (TGF-β, insulin) have been shown to impact oocyte quality, although reportedly not through germ-cell death.[27] Thus, we reasoned that a somatic aging signal may use VAB-1 to regulate physiological germ-cell apoptosis. We assessed apoptosis in cohorts of *vab-1(dx31)* and N2 wild-type adults over a period of 3 days, and found only a 7% increase in the proportion of cell deaths dependent upon *vab-1*, despite a 100% increase in total cell deaths (Figure 5a). These results argue against any substantial involvement of VAB-1 in the age-dependent increase in physiological germ cell death during early adulthood.

In addition to physiological apoptosis, there is a genotoxic germline apoptosis pathway in *C. elegans* that has been well-characterized. Double-stranded breaks in DNA resulting from exposure to ionizing radiation trigger germ-cell apoptosis, and these deaths are dependent upon the p53-related protein

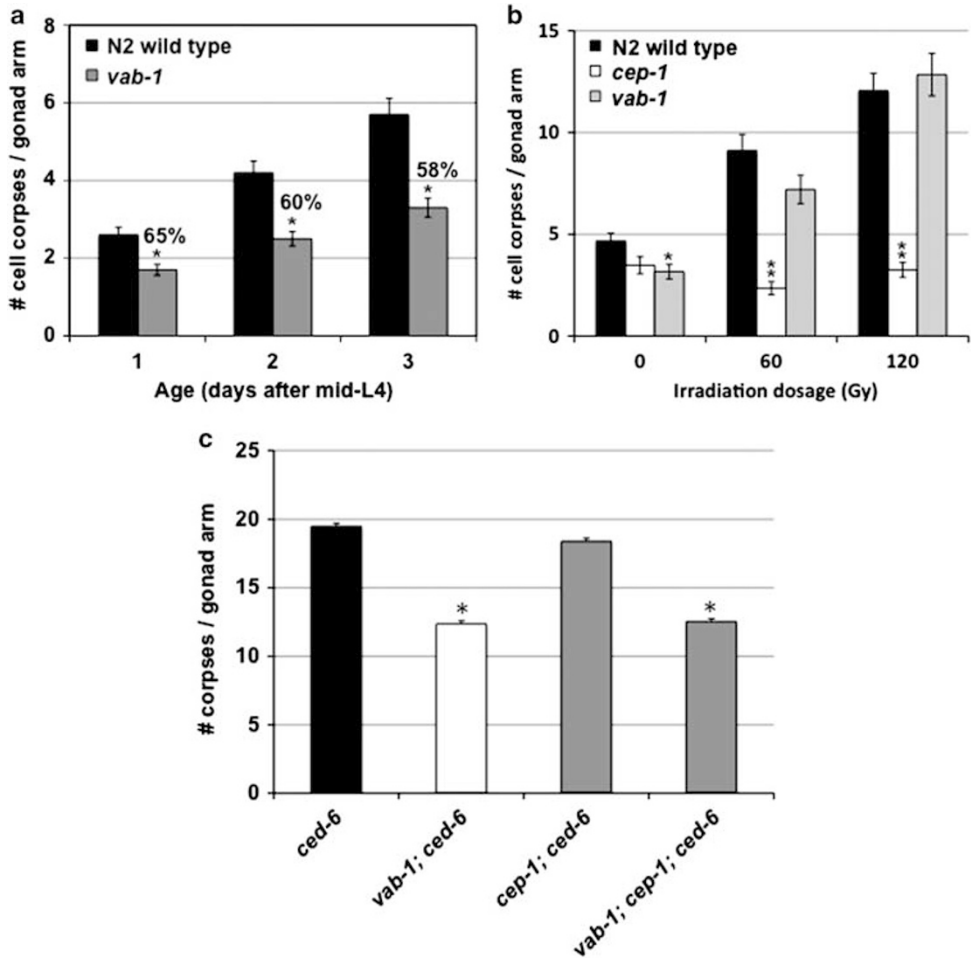

Figure 5 *vab-1* activity does not equally impact all germline cell death pathways. (**a**) Cell corpse quantification in a wild-type background over 3 days after the L4 larval stage. Apoptosis is similarly compromised in *vab-1(dx31)* mutants as animals age ($n = 40$; Mann–Whitney test with ties adjustment, $^*P < 0.001$). The numbers over the *vab-1* columns represent the percentage of corpses relative to the N2 wild-type animals at the same age. (**b**) Germ-cell corpse counts after γ-irradiation, resulting in activation of the DNA-damage pathway. A dose-dependent increase in apoptosis was lost in the *cep-1/p53(gk138)* mutant strain (*n*: all radiation doses, 29) as compared with the N2 wild type (*n*: 0 Gy, 28; 60 Gy, 29; 120 Gy, 29), but not in the *vab-1(dx31)* mutants (*n*: 0 Gy, 29; 60 Gy, 28; 120 Gy, 29; Student's *t*-test, $^{**}P < 0.001$; $^*P = 0.014$). Experiment performed under *ced-10(RNAi)* engulfment-defective conditions. (**c**) Comparison of germ-cell corpse counts between *vab-1(dx31); cep-1(gk138)* double mutants and the respective single mutant strains. All animals were *ced-6(n1813)* engulfment-defective. Loss of *cep-1* activity had no impact on corpse numbers in wild-type or *vab-1* mutant worms, while vab-1 mutants displayed reduced corpse numbers in cep-1 and wild-type animals (*n*: ced-6, 37; vab-1, 29; cep-1; ced-6, 36; vab-1; cep-1; ced-6, 39; Student's *t*-test, $^*P < 0.005$). All graphs summarize data from at least three independent experiments and represent the mean ± S.E.M.

CEP-1.[28,29] Although the trigger for this pathway is cell-intrinsic, execution of the apoptotic program in damaged cells has been shown to require somatic gene function.[17] This implied intercellular communication led us to ask whether VAB-1 was important for the DNA damage-induced germ-cell apoptosis. In *vab-1(dx31); ced-10(RNAi)* mutants, we found increased radiation exposure resulted in a dose-dependent increase in germ-cell corpse number, as in *ced-10(RNAi)* controls, demonstrating that VAB-1 does not mediate the apoptotic response to DNA damage (Figure 5b). Reciprocally, genetic analysis of *vab-1* and *cep-1* in a *ced-6(n1813)* background revealed that *cep-1* influences neither physiological cell death nor the *vab-1* cell death phenotype (Figure 5c). Together, these experiments suggest that VAB-1 and CEP-1 regulate different apoptotic events, and strengthen the conclusion that VAB-1 does not participate in intercellular signaling events required for execution of DNA damage-induced germ-cell apoptosis.

The downstream response to VAB-1 signaling in physiological apoptosis. Identification of VAB-1 as a regulator of apoptosis was sparked by the logic that ERK MAPK signaling is required for physiological germline apoptosis,[13] and the *C. elegans* ERK protein MPK-1 is subject to activation by intercellular RTK signaling in the vulva, male tail, and elsewhere.[30] We therefore asked whether VAB-1 regulates MPK-1 activation in the apoptotic region of the germline. To address this, gonads dissected from wild type and *vab-1(dx31)* mutants were immunolabeled for an activated, diphosphorylated form of MPK-1 (dpMPK-1). The data are presented in Figure 6. Consistent with other reports, we find two regions of immunoreactivity: strong fluorescence in mature oocytes, corresponding to the oocyte maturation function of MPK-1, and less intense but reproducible fluorescence preceding the gonad bend, indicative of the apoptotic function. In the apoptotic region we observed a modest decrease in the mean fluorescence and the length of the signaling zone in *vab-1* mutants, as compared with the N2 wild type, but these differences were not statistically significant. Consistent with reported downregulation of MPK-1 activity in the proximal germline, the *vab-1(dx31)* mutants showed a slight increase in mature oocytes, although this, too, was not significant.[25] While our results do not argue that VAB-1 strongly activates MPK-1 through phosphorylation in the apoptotic region of the germline, we cannot rule out a model where VAB-1 promotes apoptosis by the MPK-1 pathway.

To perform a genetic analysis of the relationship between *vab-1* and *mpk-1*, similar loss-of-function phenotypes precluded the use of epistasis tests. Consequently, we used a modified form of VAB-1 that contains a myristoylation signal (VAB-1^{MYR}), and is reported to be constitutively active.[31]

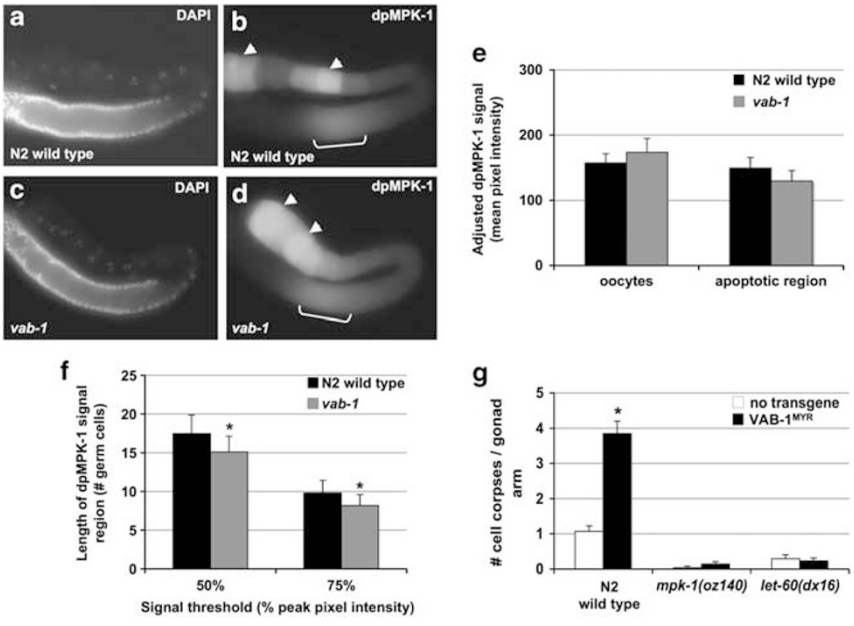

Figure 6 VAB-1/EphR and MAPK signaling. (**a–d**) Epifluorescence images of N2 wild type (**a** and **b**) and *vab-1(dx31)* (**c** and **d**) hermaphrodite gonads immunolabeled with anti-diphosphorylated MPK-1 (dpMPK-1) and counterstained with 4′,6-diamidino-2-phenylindole (DAPI). dpMPK-1 labeling was comparable in the apoptotic region of the germline (brackets) of *vab-1*-null mutants as compared with the N2 wild type, as well as in the proximal region containing mature oocytes (arrowheads). (**e**) Quantification of mean fluorescence intensity within the oocytes and the apoptotic region of dpMPK-1-immunolabeled gonads, as shown in panels **a–d**. The data represent the mean pixel intensity in a fixed area after adjustment to an anti-CGH-1 control signal (*n*: N2, 31; *vab-1*, 28). (**f**) Length of the MPK-1 apoptotic signaling zone in N2 wild-type and *vab-1(dx31)* gonads, as defined by fluorescence thresholds relative to peak fluorescence (signal $\geq$50 or 75% of local peak value). *vab-1(dx31)* had modestly shorter zones of strong dpMPK-1 labeling (Student's *t*-test, $^*P = 0.037$), and fewer *vab-1* mutants met the minimum fluorescence value for inclusion in the analysis. (**g**) Germ-cell corpse counts in N2 wild type, *mpk-1/Erk*, and *let-60/Ras* mutants with and without a transgene expressing a constitutively active, myristoylated VAB-1 receptor isoform (VAB-1^{MYR}). Apoptosis was increased upon VAB-1^{MYR} expression in the wild-type background (normal engulfment; *n*: no transgene, 30; *VAB-1^{MYR}* 39), and this increase was dependent upon both *mpk-1/Erk* (*n*: no transgene, 26; *VAB-1^{MYR}* 28) and *let-60/Ras* (*n*: no transgene, 28; *VAB-1^{MYR}* 26) function (Mann–Whitney test with ties adjustment, $^*P < 0.001$). Mutations used: *mpk-1(oz140)*, *let-60(dx16)*, and *vab-1(dx31)*. Data were collected from at least three independent experiments and represent the mean ± S.E.M.

We observed an increase in apoptosis when expression of VAB-1^{MYR} was induced in a wild-type background (Figure 6g). No increase was observed in *mpk-1(oz140)* or *let-60(dx16)* mutants, in which almost no apoptosis occurs. This result argues that VAB-1 function is dependent on MPK-1 pathway activity. A simple interpretation based on both the immunolabeling and genetic results is that physiological apoptosis can only occur in the region of MPK-1 signaling, and that apoptosis is actively promoted in parallel by VAB-1. An alternative interpretation is that VAB-1 does act through MPK-1, but that this regulation is specific to the physiological apoptosis function of MPK-1, and is not detectable by dpMPK-1 immunolabeling.

Sheath cells mediate a pro-apoptotic signal to the germline. Our EFN-3 rescue experiments suggested that somatically expressed EFNs were capable of promoting VAB-1-dependent germ-cell death. We reasoned that if EFN–EphR signaling represented an example of germ-cell murder by the overlying somatic tissue, removal of these cells would compromise signaling and lead to a reduction in germ-cell deaths.

To address this hypothesis, we performed cell ablation of the sheath cells that surround the germline syncytium. There are five sheath cell pairs surrounding the hermaphrodite germline, and sheath cell pairs 1 and 2 envelop the region of the germline in which most apoptosis takes place (Figure 1a). We found that ablation of either sheath cell pair-1 or sheath cell pair-2 in mid-late L4 *ced-6(n1318)* hermaphrodites did not impact cell death, but that ablation of both cell pairs resulted in a 42% reduction in the amount of germ-cell corpses 36 h later (35.4–20.4; Figure 7a). The decrease in germ cell death we observed is consistent with disruption of a pro-apoptotic sheath cell function, and was strikingly similar in phenotype severity to *vab-1* and *efn-1,2,3* mutants. This pro-apoptotic sheath cell function is particularly compelling, given that removal of a phagocytic cell might otherwise have been expected to result in an increased accumulation of germ-cell corpses, as is seen engulfment-defective mutants.

Next, we assessed whether interruption of VAB-1/EphR signaling could be the molecular mechanism underlying the reduced apoptosis in the sheath cell ablation experiments. We performed similar double sheath cell pair kills in *vab-1(dx31)* mutants with a wild-type engulfment background, and found that at 24 h after the L4 larval stage, ablation of the sheath cells in *vab-1* mutants did not reduce apoptosis further. This result strongly indicates that sheath cells and VAB-1 promote apoptosis in the same population of germ cells (Figure 7b), a point supported by the similar degree of cell death reduction observed in sheath-ablated and *vab-1* mutant gonads.

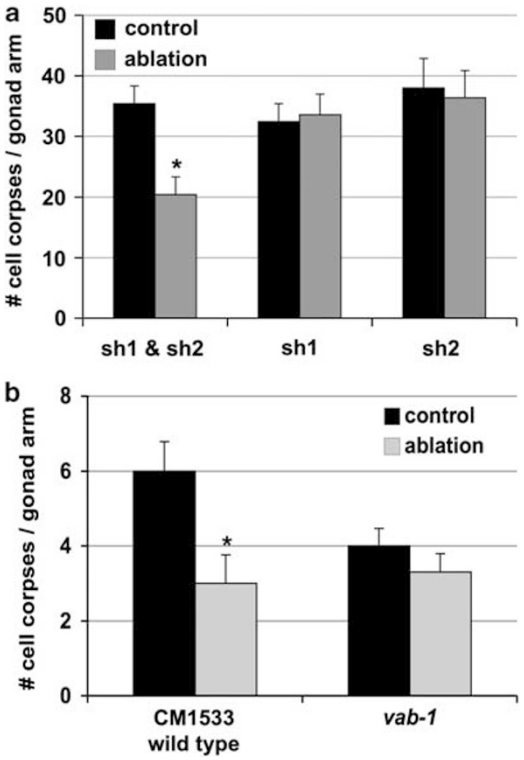

Figure 7 Gonad sheath cells function with VAB-1 to assist in physiological germ-cell death. (**a**) Germ-cell corpse counts in *ced-6(n1813)* animals 36 h after sheath cell pair-1 (sh1; $n=7$), pair-2 (sh2; $n=5$), or both (sh1 and sh2; $n=12$) were killed by laser ablation in the mid-L4 larval stage. Apoptosis in operated gonad arms (ablation; gray) was significantly reduced as compared with unoperated sister arms (control; black) when both pairs of sheath cells were killed (Student's paired *t*-test, $^*P<0.001$). (**b**) Germ-cell corpse counts 24 h after laser ablation of both sheath cell pairs in *vab-1(dx31)* mutants with a wild-type background (engulfment normal). Apoptosis was reduced in the CM1533 wild type after elimination of sheath cells ($n=9$; Student's paired *t*-test, $^*P=0.003$), as in panel **a**, but was not reduced further in the *vab-1* mutants ($n=10$). All graphs summarize data from at least three independent experiments and represent the mean ± S.E.M.

Discussion

VAB-1/EphR signaling and the gonad sheath promote apoptosis in the *C. elegans* germline. There are few known cases apart from the mammalian immune system in which one cell or tissue directs cell death in neighboring cells. Here, we present evidence for an example of such a cell murder in the *C. elegans* reproductive system. We show that the somatic gonad sheath cells promote approximately half of physiological germ-cell deaths. This function relies on an intercellular signaling event from multiple ephrin ligands to the EphR VAB-1, as evidenced by a similar partial reduction in germ-cell death in *vab-1* and *efn-1,2,3* triple mutants. Analysis of germ-cell number and germ-cell death under conditions where engulfment was blocked confirm that *vab-1* promotes apoptosis, rather than reducing germline size or enhancing cell corpse removal. Thus, this work provides evidence for a novel case of cell murder in *C. elegans*.

The reduction in germ-cell death observed after ablation of the phagocytic sheath cells was an exciting result, although the ability of these cells to impact apoptosis is not altogether surprising. While blocking the corpse engulfment process does cause an accumulation of visible germ-cell corpses, mutations in many engulfment pathway genes have been found to enhance cell survival under certain conditions,[32] and engulfment has been shown to promote another form of cell death in *C. elegans*.[33] Further, the phagocyte receptor CED-1 localizes not only to the sheath cell membrane adjacent to

apoptotic germ cells, but also surrounding cells that do not undergo apoptosis,[34] which suggests a degree of signal refinement between the apoptotic germ and phagocytic sheath cells. Together with our data, these reports provide evidence of crosstalk between cells during apoptosis, and that apoptosis and engulfment are dynamic and interconnected processes. Thus in this case, cell 'murder' may more appropriately be considered 'assisted suicide.'

Mechanism of VAB-1-dependent germ-cell death. Apart from the critical role played by engulfment pathway genes, additional somatic signals are able to influence germ-cell apoptosis non-autonomously. Neuronal secretion of TYR-2 and somatic KRI-1 activity have been implicated as pro-apoptotic regulators of *cep-1/p53*-dependent germ-cell death.[17,19] With respect to physiological germ-cell death, the transcriptional regulator LIN-35/Rb promotes apoptosis by control over expression of the core apoptotic machinery, and it is required in both the germline and the gonad sheath.[18] Interestingly, mutants for *lin-35* and other Rb complex genes show an approximately 50% decrease in germ-cell death, as we observed for *vab-1* and *efn* mutant animals. Thus, examination of *ced-3*, *ced-4*, and *ced-9* expression in *vab-1* mutants may reveal whether there is a mechanistic connection between *lin-35* and *vab-1*, or whether VAB-1/EphR signaling represents an independent somatic pathway capable of influencing the rate of physiological germ-cell death.

A fundamental question raised by this work is why a complete loss of VAB-1 function only reduces physiological germ-cell deaths by up to one half. One possible explanation is that physiological germline apoptosis in fact represents a composite of baseline activity from multiple regulatory pathways, among them the EFN–VAB-1 pathway. Indeed, several pathways capable of impacting germline apoptosis have been described.[15,16,35] Thus, it would be interesting to explore whether compromising these pathways in various combinations causes additive or synergistic physiological apoptosis deficits. An alternative model to explain the incomplete reduction of germ-cell death when VAB-1 signaling is eliminated is that this pathway acts to supplement the autonomous cell death program. A similar model has been proposed for somatic cell deaths in *C. elegans*, where neighboring phagocytes and the genes controlling engulfment promote apoptosis when core caspase signaling is reduced.[32,36] Experiments to address whether such a supplementary feedback pathway is active in the gonad sheath, and whether VAB-1 acts to initiate apoptosis or promote the process at a later step, would help to test this alternate possibility. While the mechanism remains an open question, it is clear that the EFN–VAB-1 pathway provides a modulatory, rather than essential, pro-apoptotic, signal to the germ cells under physiological conditions, and future work can elucidate how and why this modulation of germ-cell death is regulated.

Eph signaling and apoptosis. This work provides the first cellular description of an EphR-mediated cell death decision, and only the second example of pro-apoptotic Eph signaling in a normal process of animal development. Specifically, in the mouse, EphA7 signaling has been found to impact cortical brain size through positive regulation of neural progenitor apoptosis.[37] We find it noteworthy that in both the mouse and *C. elegans* examples, EphR signaling positively regulates physiological cell death decisions. In each case, EphR signaling acts as a modulator, rather than a required mediator, of apoptosis. This raises the possibility that EphR signaling may communicate pro-apoptotic physiological signals to many target cell populations. The deployment of ephrin–EphR signaling provides the potential added advantage of a bi-directional signaling system that may further synchronize apoptosis with the processes of neighboring non-apoptotic cells, such as corpse removal.[38] Experiments in other contexts will address the question of whether these disparate examples represent a conserved mechanism of physiological control over cell death, or a case of convergent evolution. In either case, the discovery of a pro-apoptotic function for VAB-1 in *C. elegans* affords a tractable model in which to address questions regarding this relatively novel function for EphR signaling.

Implications of phagocyte–target cell interactions in apoptosis. The discovery of pro-apoptotic functions for the sheath cells and VAB-1/EphR signaling has given rise to many new questions regarding VAB-1 function and the intercellular signaling events that lead to germ-cell apoptosis. Better understanding of the mechanism of VAB-1 action, the relative function of the EFN ligands, and the downstream signal transduction cascades will help to provide insight into the patterning that governs germ-cell equivalence and the survival *versus* death decision. More broadly, continued work to elucidate the integrated nature of apoptosis and phagocytosis will inform on how these processes and signals create dynamic and responsive physiological control over cell death. In particular, the description of new levels of intercellular crosstalk may open up avenues for potential intervention in clinical conditions where the dysregulation of apoptosis and/or corpse removal contributes to the etiology of disease.

Materials and Methods

***C. elegans* strains and strain construction.** Standard techniques for *C. elegans* culture and genetic manipulation were used.[39] Detailed genetic information can be found at Wormbase (http://www.wormbase.org/). Mutations used:

Linkage Group (LG)-I: *ppw-1(pk1425), rrf-1(pk1417), cep-1(gk138)*
LG-II: *vab-1(dx31), vab-1(e2), vab-1(e699), vab-1(e856), vab-1(ju8), rrf-3(pk1426)*
LG-III: *mpk-1(oz140), ced-6(n1813)*
LG-IV: *efn-1(e96), efn-2(ev658), let-60(dx16)*
LG-X: *efn-3(ev696)*

The transgenic strains used in this work include IC57: *quIs2[$P_{hsp16-41}$::myr-vab-1; rol-6^D + P_{ttx-3}::gfp]*; CM1533: *ced-6(n1813); tnIs6 [P_{lim-7}::gfp + rol-6^D]*;[40] DG2102: *unc-119(ed3); tnIs13[P_{pie-1}::vab-1::gfp::pie-1 3′UTR + unc-119(+)]*;[25] CM2081: *efn-1(e96), efn-2(ev658); efn-3(ev696); guEx1299 [P_{pie-1}::efn-3 + P_{myo-2}::GFP]*; CM2082: *efn-1(e96), efn-2(ev658); efn-3 (ev696); guEx1300[P_{lim-7}::efn-3 + P_{myo-2}::gfp]*; and MD701: *bcIs39 [P_{lim-7}::CED-1::GFP + lin-15(+)]*.

To generate an inducible, activated VAB-1, we incorporated the c-Src N-terminal myristoylation signal (MGSSKS) in VAB-1 using a PCR-based approach. A forward primer (oIC-101) encoding the myristoylation signal sequence and sequences to *vab-1* was used with a reverse primer to the 3′ end of *vab-1* (oAC-428) to amplify a 1.6-kb cDNA encoding the intracellular portion of VAB-1 (585 aa–1117 aa).

This fragment was cloned into the *Nhe*I/*Kpn*I sites of pPD49.83 (*hsp 16–41*) and termed pIC30. N2 worms were injected with 70 ng/μl pIC30, 30 ng/μl pRF4 (*rol-6* dominant), 30 ng/μl and P_{ttx-3}::*GFP*. Extrachromosomal array lines were obtained and a stable chromosomal integration by exposure to UV light was used to establish *quIs2*.[41]

For construction of *efn-3*-expressing transgenes, we PCR-amplified the full-length *efn-3* cDNA (636 bp) with restriction sites engineered into the 5′ ends of primers specific to the cDNA ends. P_{pie-1}::*efn-3* was constructed by cloning an *efn-3* amplicon (PR2569 + PR2570) into the *Bam*HI sites of pJH4.66 (P_{pie-1}::*TBB-1*[42]), and named pRJ112. To construct a transgene with sheath cell-specific *efn-3* expression, we amplified a 160-bp fragment containing the sheath cell response element from *lim-7* by nested PCR (PR2541 + PR2544; PR2542 + PR2543).[40] This fragment was cloned into the *Xba*I/*Pst*I sites of a pPD49.26 vector (gift from A Fire) containing an *efn-3* cDNA sequence, and termed pRJ104. N2 worms were injected with 20 ng/μl pRJ112 or pRJ104, 10 ng/μl P_{myo-2}::*gfp*, and 70–90 ng/μl yeast genomic DNA. Extrachromosomal array lines were obtained, established as *guEx1299* (P_{pie-1}::*efn-3)* and *guEx1300* (P_{lim-7}::*efn-3)*, and scored in the first few generations to limit the effects of extrachromosomal transgene suppression. All primer sequences are available upon request.

Apoptosis assays. Cell corpses were identified for their refractile, button-like morphology, according to previous methods.[13] Unless otherwise noted, cohorts of mid-stage L4 larval hermaphrodites were selected and plated on standard nematode growth medium (NGM) plates for overnight growth at 20 °C. Animals were scored or processed for scoring 24 h after L4 plating, unless otherwise noted. Strains carrying the IC57 (*quIs2*; *hsp*::*myr*::*vab-1*) transgene were raised to ~34 h after L4 stage, subjected to 35 °C for 1 h, recovered 1 h, and scored directly under Normarski optics.

All animals were scored by Nomarski optics, and most were further scored for incorporation of the vital DNA dye SYTO12 (Invitrogen, Carlsbad, CA, USA), which preferentially binds to DNA fragments in apoptotic cells. Experiments in which SYTO12 staining was performed were performed as described previously.[13] Several assays were performed under different experimental conditions or cell engulfment-defective backgrounds (*ced-6* mutant or *ced-10* RNAi knockdown). Consequently, the average number of germ-cell corpses observed in the wild type varies based on the experimental background presented. However, in all cases assessment of a wild-type control in parallel to the experimental animals provides an appropriate internal comparison. All germ-cell corpse data were gathered from multiple independent experiments, and presented as mean ± S.E.M.

Irradiation-induced DNA damage. L4 hermaphrodites were seeded onto NGM plates and positioned above a Cobalt-60 γ-irradiation source (provided by the OSU Nuclear Reactor Lab, Columbus, OH, USA). Animals were exposed for periods of time calculated to generate 0, 60, and 120 Gy units of γ-ray exposure. Animals were recovered and transferred to *ced-10(RNAi)* plates for overnight growth and germ-cell corpse scoring. Data were collected from three independent experiments.

Germ-cell quantification. Mid-stage L4 hermaphrodites were plated on standard NGM plates for overnight growth at 20 °C. For animals not subjected to heat shock, gonads were excised after 24 h of growth, fixed for 15–30 min in 4% paraformaldehyde, washed 3 × with 1 × PBS, 0.1% Tween-20 (pH 7.4) (PBST), and stained for 5 min in 2 μg diamidinophenylimidazole (DAPI) per ml PBST.

DAPI-stained gonads were visualized by immunofluorescence microscopy at × 400 magnification. Z-stack image series were captured, compiled, false-colored, and annotated using Adobe Photoshop software. Germ-cell counts for each gonad were manually counted in small sections from processed Z-stack image data; 3–4 animals of each genotype were scored from each of three independent experiments. Germ-cell zones were called according to nuclear morphology, with the transition zone being defined distally by the first dense crescent-shaped chromatin bodies and proximally by the predominance of 'bowl of spaghetti' nuclei indicative of the pachytene stage. The oocyte–pachytene boundary was defined by the appearance linearly arranged single germ cells.

Immunohistochemistry and quantification of activated MPK-1. Adult hermaphrodite gonads were dissected according to a standard protocol.[43] Cohorts of ~50 dissected animals/gonads were fixed 1 h with 4% paraformaldehyde in a 20 mM K_2PO_4 (pH 7.2). Gonads were then post-fixed for 5 min in cold 100% MeOH. After two washes in PBST + 30% goat serum, gonads were left in a third PBST/serum wash as a blocking solution for 1 h at room temperature. Gonads were incubated with a primary antibody overnight at 4 °C. On day 2, gonads were washed 4 × with PBST/serum and incubated with the secondary antibody for 4 h at room temperature. Next, gonads were washed 4 × in PBST, stained with 2 μg DAPI per ml PBST. Gonads were washed 1 × with PBST and mounted on glass slides using the Slowfade antifade reagent (Invitrogen). The antibody concentrations used were as follows: 1 : 200 mouse anti-diphosphorylated ERK-1/-2 (clone MAPK-YT; Sigma-Aldrich, St. Louis, MO, USA), 1 : 1000 rabbit anti-CGH-1 (gift from D Greenstein), 1 : 200 goat anti-rabbit IgG-Cy3 (Sigma-Aldrich), and 1 : 200 sheep anti-mouse FITC (Sigma-Aldrich).

RNA interference. For both cell corpse engulfment-defective apoptosis assays and VAB-1 site-of-action experiments, animals were subjected to feeding RNAi.[44] Fresh overnight cultures of *Escherichia coli* strain HT115 bearing pRJ110 (*ced-10* cDNA in pPD129.36), pRJ113 (*vab-1* cDNA in pPD129.36), or pPD129.36 (control) were spotted onto NGM plates supplemented with 1 mM IPTG and 25 mg/ml carbenicillin. The plates were left at room temperature overnight, and seeded with L4 hermaphrodites the following day.

Cell ablation. L4 hermaphrodites were subject to laser ablation of gonad sheath cells, according to established methods.[45] Animals were anesthetized on 3% agar slides in an M9 solution containing 25 mM levamisole. Slides were placed on a Zeiss AxioSkop II (Carl Zeiss, Thornwood, NY, USA), fitted with a VSL-337 laser (Laser Sciences, Newton, MA, USA) with MicroPoint attachment (Photonic Instruments, Arlington Heights, IL, USA). The full genotype of the strains for this experiment was as follows: CM1533: *ced-6(n1813); tnIs6*, and CM2083: *vab-1(dx31); ced-6(n1813); tnIs6.* The gonadal sheath cells were identified based on their morphology, position, and expression of P_{lim-7}::*GFP*, and killed under Nomarski optics. Cells of either the anterior or the posterior gonad were ablated in late L4-stage hermaphrodites, allowing the intact arm to serve as a matched internal control. Animals were allowed to recover on standard NGM plates at 20 °C prior to apoptosis scoring. Killing of the sheath cells was confirmed, and germ-cell corpses were scored 24 or 36 h later.

Conflict of Interest

The authors declare no conflict of interest.

Acknowledgements. We thank Hongtao Jia for helpful discussions and preliminary experiments, and Steven Billups, Mark Corkins, and Elizabeth Ulm for comments on the manuscript. Some nematode strains used in this work were provided by the Caenorhabditis Genetics Center, which is funded by the NIH National Center for Research Resources (NCRR). Work in the Chamberlin lab is supported by the National Science Foundation (NSF).

1. Kerr JF, Wyllie AH, Currie AR. Apoptosis: a basic biological phenomenon with wide-ranging implications in tissue kinetics. *Br J Cancer* 1972; **26**: 239–257.
2. Fadeel B, Orrenius S. Apoptosis: a basic biological phenomenon with wide-ranging implications in human disease. *J Intern Med* 2005; **258**: 479–517.
3. Gurzov EN, Eizirik DL. Bcl-2 proteins in diabetes: mitochondrial pathways of $\hat{I}^2$-cell death and dysfunction. *Trends Cell Biol* 2011; **21**: 424–431.
4. Ruffin N, Ahmed SS, Osorio LM, Wang XN, Jackson GH, Collin MP *et al.* The involvement of epithelial Fas in a human model of graft *versus* host disease. *Transplantation* 2011; **91**: 946–951.
5. Brumatti G, Salmanidis M, Ekert PG. Crossing paths: interactions between the cell death machinery and growth factor survival signals. *Cell Mol Life Sci* 2010; **67**: 1619–1630.
6. Stupack DG, Cheresh DA. Get a ligand, get a life: integrins, signaling and cell survival. *J Cell Sci* 2002; **115** (Pt 19): 3729–3738.
7. Guicciardi ME, Gores GJ. Life and death by death receptors. *FASEB J* 2009; **23**: 1625–1637.
8. O'Reilly LA, Tai L, Lee L, Kruse EA, Grabow S, Fairlie WD *et al.* Membrane-bound Fas ligand only is essential for Fas-induced apoptosis. *Nature* 2009; **461**: 659–663.
9. Chavez-Galan L, Arenas-Del Angel MC, Zenteno E, Chavez R, Lascurain R. Cell death mechanisms induced by cytotoxic lymphocytes. *Cell Mol Immunol* 2009; **6**: 15–25.
10. Gartner A, Boag PR, Blackwell TK. Germline survival and apoptosis. *WormBook* 2008 (http://www.wormbook.org).
11. Baum JS, St George JP, McCall K. Programmed cell death in the germline. *Semin Cell Dev Biol* 2005; **16**: 245–259.
12. Wolke U, Jezuit EA, Priess JR. Actin-dependent cytoplasmic streaming in *C. elegans* oogenesis. *Development* 2007; **134**: 2227–2236.
13. Gumienny TL, Lambie E, Hartwieg E, Horvitz HR, Hengartner MO. Genetic control of programmed cell death in the *Caenorhabditis elegans* hermaphrodite germline. *Development* 1999; **126**: 1011–1022.

14. Hubbard EJA, Greenstein D. Introduction to the germ line. *WormBook* 2005 (http://www.wormbook.org).
15. Boag PR, Nakamura A, Blackwell TK. A conserved RNA–protein complex component involved in physiological germline apoptosis regulation in *C. elegans*. *Development* 2005; **132**: 4975–4986.
16. Salinas LS, Maldonado E, Navarro RE. Stress-induced germ cell apoptosis by a p53 independent pathway in *Caenorhabditis elegans*. *Cell Death Differ* 2006; **13**: 2129–2139.
17. Ito S, Greiss S, Gartner A, Derry WB. Cell-nonautonomous regulation of *C. elegans* germ cell death by kri-1. *Curr Biol* 2010; **20**: 333–338.
18. Schertel C, Conradt B. *C. elegans* orthologs of components of the RB tumor suppressor complex have distinct pro-apoptotic functions. *Development* 2007; **134**: 3691–3701.
19. Sendoel A, Kohler I, Fellmann C, Lowe SW, Hengartner MO. HIF-1 antagonizes p53-mediated apoptosis through a secreted neuronal tyrosinase. *Nature* 2010; **465**: 577–583.
20. Reinke V, Gil IS, Ward S, Kazmer K. Genome-wide germline-enriched and sex-biased expression profiles in *Caenorhabditis elegans*. *Development* 2004; **131**: 311–323.
21. Wang X, Roy PJ, Holland SJ, Zhang LW, Culotti JG, Pawson T. Multiple ephrins control cell organization in *C. elegans* using kinase-dependent and -independent functions of the VAB-1 Eph receptor. *Mol Cell* 1999; **4**: 903–913.
22. Schumacher B, Schertel C, Wittenburg N, Tuck S, Mitani S, Gartner A *et al*. *C. elegans* ced-13 can promote apoptosis and is induced in response to DNA damage. *Cell Death Differ* 2005; **12**: 153–161.
23. Chin-Sang ID, Moseley SL, Ding M, Harrington RJ, George SE, Chisholm AD. The divergent *C. elegans* ephrin EFN-4 functions in embryonic morphogenesis in a pathway independent of the VAB-1 Eph receptor. *Development* 2002; **129**: 5499–5510.
24. Hahn AC, Emmons SW. The roles of an ephrin and a semaphorin in patterning cell–cell contacts in *C. elegans* sensory organ development. *Dev Biol* 2003; **256**: 379–388.
25. Cheng H, Govindan JA, Greenstein D. Regulated trafficking of the MSP/Eph receptor during oocyte meiotic maturation in *C. elegans*. *Curr Biol* 2008; **18**: 705–714.
26. Andux S, Ellis RE. Apoptosis maintains oocyte quality in aging *Caenorhabditis elegans* females. *PLoS Genet* 2008; **4**: e1000295.
27. Luo S, Kleemann GA, Ashraf JM, Shaw WM, Murphy CT. TGF-beta and insulin signaling regulate reproductive aging via oocyte and germline quality maintenance. *Cell* 2010; **143**: 299–312.
28. Schumacher B, Hofmann K, Boulton S, Gartner A. The *C. elegans* homolog of the p53 tumor suppressor is required for DNA damage-induced apoptosis. *Curr Biol* 2001; **11**: 1722–1727.
29. Derry WB, Putzke AP, Rothman JH. *Caenorhabditis elegans* p53: role in apoptosis, meiosis, and stress resistance. *Science* 2001; **294**: 591–595.
30. Sundaram MV. RTK/Ras/MAPK signaling. *WormBook* 2006 (http://www.wormbook.org).
31. Mohamed AM, Chin-Sang ID. Characterization of loss-of-function and gain-of-function Eph receptor tyrosine kinase signaling in *C. elegans* axon targeting and cell migration. *Dev Biol* 2006; **290**: 164–176.
32. Hoeppner DJ, Hengartner MO, Schnabel R. Engulfment genes cooperate with ced-3 to promote cell death in *Caenorhabditis elegans*. *Nature* 2001; **412**: 202–206.
33. Galvin BD, Kim S, Horvitz HR. *Caenorhabditis elegans* genes required for the engulfment of apoptotic corpses function in the cytotoxic cell deaths induced by mutations in lin-24 and lin-33. *Genetics* 2008; **179**: 403–417.
34. Wang X, Li W, Zhao D, Liu B, Shi Y, Chen B *et al*. *Caenorhabditis elegans* transthyretin-like protein TTR-52 mediates recognition of apoptotic cells by the CED-1 phagocyte receptor. *Nat Cell Biol* 2010; **12**: 655–664.
35. Angelo G, Van Gilst MR. Starvation protects germline stem cells and extends reproductive longevity in *C. elegans*. *Science* 2009; **326**: 954–958.
36. Reddien PW, Cameron S, Horvitz HR. Phagocytosis promotes programmed cell death in *C. elegans*. *Nature* 2001; **412**: 198–202.
37. Depaepe V, SuarezGonzalez N, Dufour A, Passante L, Gorski JA, Jones KR *et al*. Ephrin signalling controls brain size by regulating apoptosis of neural progenitors. *Nature* 2005; **435**: 1244–1250.
38. Pasquale EB. Eph–ephrin bidirectional signaling in physiology and disease. *Cell* 2008; **133**: 38–52.
39. Sulston JE, Schierenberg E, White JG, Thomson JN. The embryonic cell lineage of the nematode *Caenorhabditis elegans*. *Dev Biol* 1983; **100**: 64–119.
40. Voutev R, Keating R, Hubbard EJA, Vallier LG. Characterization of the *Caenorhabditis elegans* islet LIM-homeodomain ortholog, lim-7. *FEBS Lett* 2009; **583**: 456–464.
41. GengyoAndo K, Mitani S. Characterization of mutations induced by ethyl methanesulfonate, UV, and trimethylpsoralen in the nematode *Caenorhabditis elegans*. *Biochem Biophys Res Commun* 2000; **269**: 64–69.
42. Strome S, Powers J, Dunn M, Reese K, Malone CJ, White J *et al*. Spindle dynamics and the role of gamma-tubulin in early *Caenorhabditis elegans* embryos. *Mol Biol Cell* 2001; **12**: 1751–1764.
43. Lee M, Schedl T. RNA *in situ* hybridization of dissected gonads. *WormBook* 2006 (http://www.wormbook.org).
44. Timmons L, Court DL, Fire A. Ingestion of bacterially expressed dsRNAs can produce specific and potent genetic interference in *Caenorhabditis elegans*. *Gene* 2001; **263**: 103–112.
45. Kimble J. Alterations in cell lineage following laser ablation of cells in the somatic gonad of *Caenorhabditis elegans*. *Dev Biol* 1981; **87**: 286–300.